https://ntrs.nasa.gov/search.jsp?R=20170000881 2020-05-09T18:07:23+00:00Z

Parallel Hybrid Gas-Electric Geared Turbofan Engine Conceptual Design and Benefits Analysis

Authors:

Charles Lents[1], Larry Hardin[2], Jonathan Rheaume[3]
United Technologies Research Center, East Hartfod, CT, 06108

and

Lee Kohlman[4]
NASA Glenn Research Center, Hampton, VA, 23681

The conceptual design of a parallel gas-electric hybrid propulsion system for a conventional single aisle twin engine tube and wing vehicle has been developed. The study baseline vehicle and engine technology are discussed, followed by results of the hybrid propulsion system sizing and performance analysis. The weights analysis for the electric energy storage & conversion system and thermal management system is described. Finally, the potential system benefits are assessed.

Nomenclature

ADP	aero design point
Alt	altitude
AOC	air oil cooler
Bat	battery
BPR	bypass ratio
Brg	bearings
cGTF	conventional geared turbofan
CoO	concept of operations
CORSZ	core corrected flow (lbm/sec)
DOC	direct operating cost
EES&C	electric energy storage and conversion
ETAC	core thermal efficiency
Fan DS	Fan Drive System
FOC	fuel oil cooler
FP	fuel pump
FPR	fan pressure ratio
Gbx	gearbox
GTF	geared turbofan
hGTF	hybrid geared turbofan
HS	high spool
ISA	international standard atmosphere
L/D	lift/drag ratio
LH2	liquid hydrogen

[1] Principal Engineer, Thermal Management Group, Thermal & Fluid Sciences Department, United Technologies Research Center, 411 Silver Lane, MS 129-89, East Hartford CT 06108, AIAA Senior Member
[2] Staff Engineer, Aerodynamics Group, Thermal & Fluid Sciences Department, United Technologies Research Center, 411 Silver Lane, MS 129-89, East Hartford CT 06108, AIAA Senior Member
[3] Senior Engineer, Thermal Management Group, Thermal & Fluid Sciences Department, United Technologies Research Center, 411 Silver Lane, MS 129-89, East Hartford CT 06108
[4] Research Aerospace Engineer, Rotating and Drive Systems Branchy, Glenn Research Center, 1 North Dryden Street, MS 442, Hampton VA 23681, AIAA Member

LS	low spool
Mach	mach number
MCL	maximum climb thrust
MCR	maximum cruise
MD	motor drive
MG	motor/generator
MTO	maximum takeoff
OPR	operating pressure ratio
PEM FC	proton exchange membrane fuel cell
RCC	ram coolant cooler
SG	starter-generator
SLS	Sea Level Static
SUGAR	subsonic ultra green aircraft research
TAMB	temperature above standard ambient (°F)
TMS	thermal management system
TOGW	takeoff gross weight
TSFC	thrust specific fuel consumption (lbm/hr/hp)
T4	turbine inlet temperature (°F)

I. Introduction

This NASA-funded program has produced the notional concept of operations and conceptual design of a parallel gas-electric hybrid propulsion system. The study has been constrained to a conventional single aisle twin engine tube and wing vehicle. Additionally, the propulsion system architecture has been constrained to a conventional high bypass ratio propulsor where the propulsion fan can be driven by both the low pressure turbine and a fan spool-mounted motor/generator. In the selected concept of operations (CoO), the low spool (LS) motor/generator is used as a motor for boost power during takeoff and climb only, enabling the engine core to be sized at the MCR (maximum cruise) condition. During cruise, the LS motor/generator can be operated in generate mode to charge the batteries for idle descent, ground idle or for the next mission takeoff and climb segment. The subsystems' electric power needs are met by stored electric power when the LS motor/generator is in motor mode and by the LS motor/generator when it is not being used as a motor, i.e., in generate mode. This CoO selection drove the remaining propulsion system design parameters. The hybrid geared turbofan (GTF) (hGTF) with a core sized for cruise has the same MCR overall pressure ratio (OPR) (59.8) as a conventional GTF (cGTF), but with a 17% smaller core flow. With the smaller core, the hGTF requires a 2.1 MW motor to provide required takeoff thrust. 1495 kW-hrs of stored energy are required by both engines for the takeoff and climb segments.

With current technology batteries (170 W-hr/kg), electric components and thermal management system components, an hGTF-based airplane has much higher mission fuel burn than a cGTF based airplane for a 900 nm direct operating cost (DOC) mission. However, with improvements in electric components power density and thermal management systems capability, a ~ 5% reduction in Jet-A fuel consumption for the DOC mission is possible.

II. Study Baseline Vehicle and Engine

The baseline vehicle is the Boeing defined N+4 2035 Refined SUGAR [1,2] airframe powered by a second generation conventional GTF (cGTF) engine. This is a conventional tube and wing vehicle with wing span constrained to fit between gates as configured today. Advanced materials for a lightweight, high L/D airframe are assumed. A comparison between a modern single aisle 737-800 reference and the Refined SUGAR baseline airframe is provided in Table 1 and **Error! Reference source not found.**.

Table 1: 737 Compared to Refined SUGAR N+4 Airframe

Sizing Level	737-800 Reference	N+4 Refined Sugar Baseline
Passengers/Class	154/DUAL	154/DUAL
Max Takeoff Gross Weight (lbm)	174200	136412
Operating Empty Weight (lbm)	91660	79213
Fuel Capacity (lbm)	46063	26513
Wing Area (ft^2)	1341	1,358

Aspect Ratio (Effective)	9.45	11.07
Cruise L/D @ Optimal CL	17.7	21.5
Design Mission Range (nm)	3,149	3,149
DOC Mission Range (nm)	900	900
Cruise Mach	0.79	0.74

Figure 1: 737 Compared to Refined SUGAR N+4 Airframe

The choice of a second generation GTF for the baseline vehicle is driven by the long horizon 2035 entery into service for the baseline vehicle. The cGTF has been sized for the baseline refined SUGAR aircraft. Design and performance parameters are provided in Table 2.

Table 2: cGTF Design and Performance Parameters

	Alt (kft)	Mach	ΔT_{AMB} (F)	Req Thrust	Actual Thrust	TSFC	Norm CORSZ	OPR	FPR	BPR	Norm T4	ETAC
ADP	35	0.74	0	3145	3145	0.480	1.01	55.2	1.29	18.1	0.85	0.527
MCL	35	0.74	18	3930	3930	0.499	1.00	64.6	1.35	17.0	0.96	0.535
MTO	0	0.25	27	16592	17046	0.301	0.97	54.3	1.28	18.6	1.00	0.503
SLS	0	0	27	21943	23894	0.204	0.97	51.6	1.27	18.1	0.97	0.494
MCR	35	0.74	0	3538	3538	0.479	1.01	59.8	1.32	17.6	0.89	0.535

ADP – Aero Design Point, MCL – Maximum Climb Thrust, MTO – Maximum Takeoff Thrust, SLS – Sea Level Static, MCR – Maximum Cruise Thrust, Alt – altitude, Mach – mach number, ΔTAMB – temperature above standard ambient (F), TSFC – thrust specific fuel consumption (lbm/hr/hp), CORSZ – core corrected flow (lbm/sec), OPR – operating pressure ratio, FPR – fan pressure ratio, BPR – bypass ratio, T4 – turbine inlet temperature (F), ETAC – Core thermal efficiency

III. Propulsion System Sizing and Performance Analysis General Guidelines

The architecture of a cGTF drives the engine design point to occur at takeoff or top of climb. To make required thrust at these points, the engine core is run at the maximum T4 (turbine inlet temperature) limit, where peak efficiency is achieved. This condition also sizes engine core flow. As a result, at cruise the engine is run significantly below the long life maximum T4 limit. By adding external power during takeoff and climb to the low spool, the engine can be designed for higher T4 at the cruise condition which will improve the core efficiency.

For consistency of comparison, the FPR for the hGTF is set at the same values as that for the cGTF, as the hGTF electric boost capability has not been found to provide any low FPR enabling advantage over the cGTF. Other parameters, BPR, T4 and core size namely, have been optimized specifically for each engine. Four sizing points conditions are considered in the design of a propulsion system; 1) ADP - the aerodynamic design point which is cruise at 35k feet in a standard atmosphere, 2) MCL - max climb thrust at the same altitude and Mach number as the ADP but with the temperature at ISA+18F, 3) MTO - max takeoff thrust at sea level, M=0.25, ISA+27F, 4) SLS - sea level static thrust at ISA+27F). The cGTF engine is sized as follows.

1. The fan area is set to give a target corrected flow per unit area at the MCL sizing point.

2. The core flow is set so that T4 limits are not exceeded at MCL, MTO, or SLS. For the cGTF, the MCL sizing point sets the core flow, and T4 at MTO and SLS are slightly below the limits.

For the hybrid GTF, the procedure is slightly different. **Error! Reference source not found.** provides the results of the sizing study.

1. The fan area is set to give a target corrected flow per unit area at the MCL sizing point. This area will be slightly different than for the cGTF because the smaller core enabled by adding electric power for takeoff and climb will yield a higher bypass ratio. Notice that both the cGTF and hGTF bars of Figure 2 for MCL are at the T4/T4max limit. This shows that MCL is the sizing point for the cGTF. For the hGTF, this is by design as explained in Step 3 below.
2. The core flow is set so that with no additional low spool power T4, does not exceed the MCL T4 limit at MCR (MCR thrust is defined as 93% of the MCL thrust). Notice in Figure 2 that this MCL T4/T4max limit of 0.96 is less than the absolute T4/T4max limit of 1.0 which occurs at max takeoff. This is because MCL and MCR can occur over an extended time, so a lower T4 limit is imposed at these conditions. The MCL T4/T4max limit is used at MCR conditions as the engine is not expected to cruise at the max cruise condition very often. This procedure yields a smaller core that will not produce enough power to drive the fan at takeoff and climb conditions.
3. Once the engine has been sized, the takeoff and climb segments are considered. The T4/T4max is set at the limit (1.0 at max takeoff and 0.96 at max climb) and the developed thrust is determined. As a result, the hGTF MTO and MCL bars are at exactly the T4/T4Max limits. Power is then added to the low spool until the thrust developed by the cGTF is achieved. This determines the maximum added power required and thus provides the rating for the low spool motor/generator. For climb points between MTO and MCL, a power addition schedule is developed that closely replicates the climb thrust of the cGTF. As it turns out, this schedule is a simple linear function of altitude.

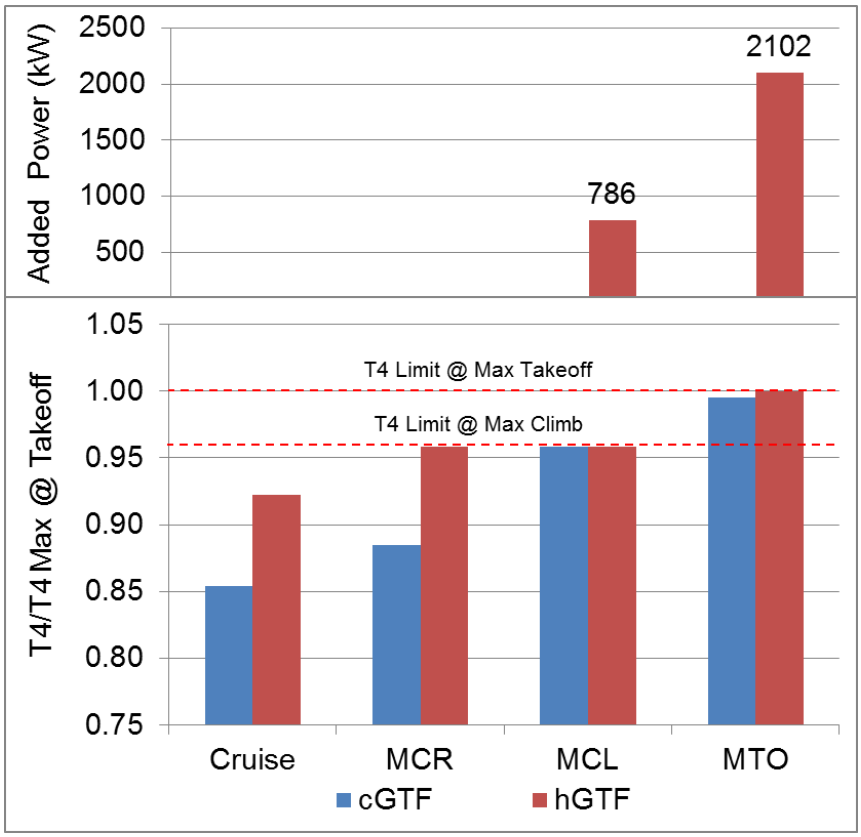

Figure 2: hGTF Sizing Results

Error! Reference source not found. shows that the added power required to make thrust at the T4 limited points of MTO and MCL are 2102 kW and 786 kW respectively. Thus, a 2102 kW motor is required for the hGTF propulsion system. With the hGTF engine size at higher T4/T4max than the conventional GTF for cruise operation, the engine achieves a lower TSFC at cruise. **Error! Reference source not found.** provides a normalized comparison. The improvement is estimated at ~ 2.3%. TSFC is also reduced at takeoff and climb, but this is primarily due to the power added to the low spool power by the low spool motor/generator.

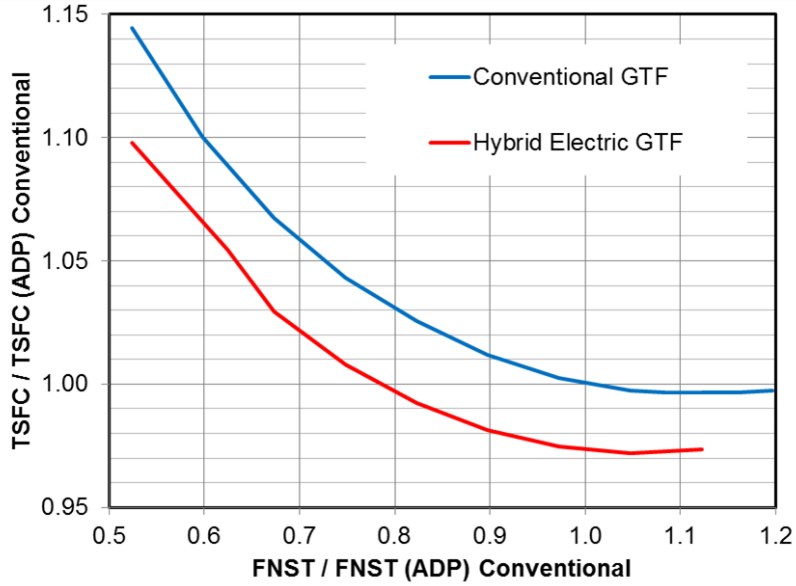

Figure 3: TSFC Improvement at Cruise for hGTF

The design and performance parameters of the hGTF engine resulting from this design procedure are provided in Table 3. Comparing Table 2 and Table 3, the notable differences between the hGTF and cGTF are BPR (21.7 v 17.6 at MCR) and core size (0.84 v 1.01 at MCR), as well as the TSFC (0.250 v 0.301 at MTO, 0.419 v 0.499 MCL, and 0.468 v 0.479 at MCR).

Table 3: hGTF Design and Performance Parameters

	Alt (kft)	Mach	ΔT_{AMB} (F)	Req Thrust	Actual Thrust	TSFC	Norm CORSZ	OPR	FPR	BPR	T4 (F)	ETAC
ADP	35	0.74	0	3145	3145	0.467	0.85	55.1	1.29	22.4	0.92	0.539
MCL	35	0.74	18	3930	3930	0.419	0.86	62.2	1.35	21.0	0.96	0.635
MTO	0	0.25	27	16592	16592	0.250	0.82	51.3	1.28	22.9	1.00	0.602
SLS	0	0	27	21943	23894	0.165	0.82	48.0	1.27	22.4	0.97	0.603
MCR	35	0.74	0	3538	3538	0.468	0.84	59.8	1.32	21.7	0.96	0.546

IV. System Weights

The propulsion system analysis provides the performance benefit of the hGTF propulsion system. Balancing this benefit is the weight penalty incurred by implementing the system. The two major sub-systems adding to system weight are the Electric Energy Storage & Conversion Systems (EES&CS) and the Thermal Management System (TMS).

A. Electric Energy Storage & Conversion (EES&C) System

The electric energy storage requirements are derived from the takeoff and climb requirements, where the electric energy storage system must provide boost power to the propulsion system, and provide primary power to the subsystems, and TMS. There is also electrical energy required during the step climb of the capability mission. This energy could come from ground power or from the LS motor/generator during the first cruise segment, where the

propulsion system could be used to charge the battery. The former option requires more battery capacity/weight and the latter requires slightly more Jet-A fuel burn during cruise. Only the stored energy required for takeoff and climb is used for battery weight estimates. **Error! Reference source not found.** provides the stored energy requirement during takeoff and climb (left chart) and step climb (right chart). 1295 kW-hr is required at the low spool to provide boost power to the fan during takeoff and climb, but 1495 kW-hr is required at the stored energy system output to overcome motor, motor drive and feeder losses, and to supply the subsystems power. The subsystems are powered by the battery during takeoff and climb. The motor, motor drive and feeder efficiencies are the 10 year horizon values provide in middle column of the component performance data section (left data table) of Table 4.

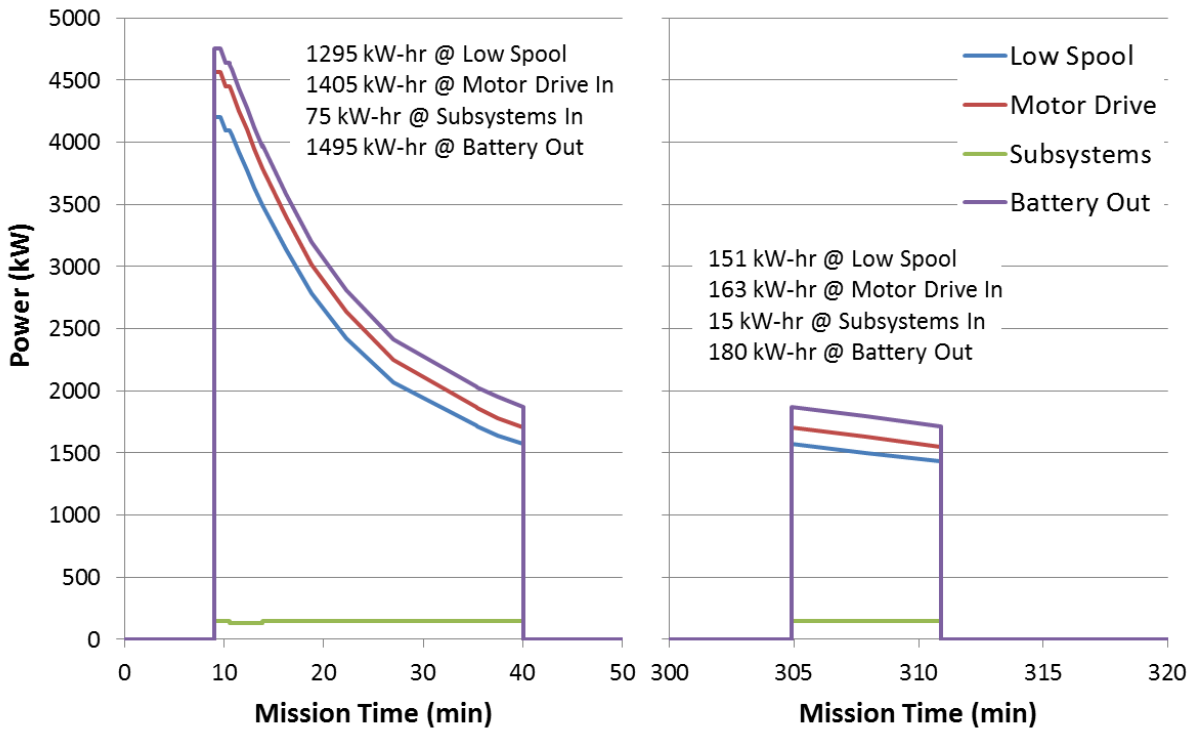

Figure 4: Stored Energy Requirements for the hGTF Based Aircraft

This analysis has been executed with the propulsion system providing max rated power at takeoff and climb. With a conventional gas turbine engine, minimal fuel burn results from a steep rapid climb so that cruising altitude is reached as soon as possible. The takeoff length is shorter and climb rate are even steeper for the shorter 900 nm DOC mission; but again for a cGTF airplane this mode of operation results in the lowest fuel burn. For the hGTF aircraft flying the 900 nm DOC mission, this scenario requires large motor boost power, but over a shorter time. A longer, more gradual climb requires less motor boost power, but over a longer time. An optimal may exist that reduces the battery storage energy requirement for the DOC mission. This will be considered in future studies. Note that this trade will not affect motor and motor drive size as they are sized to provide the needed boost power for the 3300 nm capability mission. Additionally, the analysis above provides the stored energy required for the capability mission. If a different optimal stored energy exists for the DOC mission, then removable battery packs would be required to realize the benefit.

The EES&C system must provide 2102 kW to each propulsion system and 148 kW to the subsystems during takeoff. This results in a maximum required power from the stored energy source of 4758 kW ((2102 * 2 / 0.94/ 0.98 + 148) / 0.99). The EES&C system must also have a stored energy capability of 1495 kW-hr at the stored energy source output. Providing this capability with a hydrogen fueled PEM fuel cell (both liquid H_2 and compressed H_2) or a Li-ion battery (@ 200 W-hr/kg) is compared in Figure 5. Reference 3 provides a comprehensive energy density data set for various energy storage devices and systems. A sulfur free Jet-A fueled solid oxide fuel cell has also been considered, but at the required energy storage the system weight is ~ 48,000 kg or ~ 5x heavier than the Li-ion option.

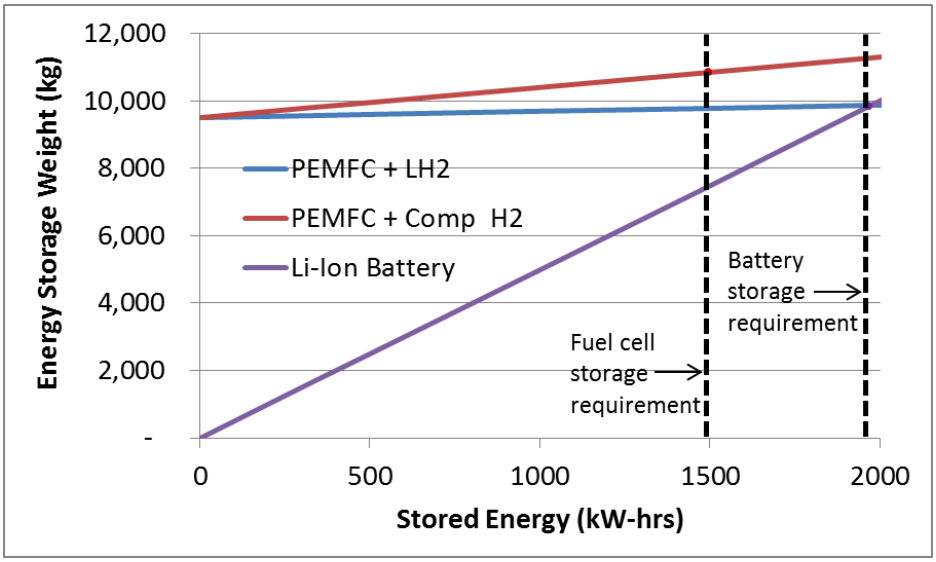

Figure 5: Weight Comparison between Li-Ion Battery and PEM Fuel Cell

Notice that the battery storage requirement is 1967 kW-hr as opposed to that for the fuel cell at 1495 kW-hr. This is because a battery cannot be fully discharged. It is assumed that with current technology the battery cannot be discharged to more than 20% of full charge. In addition, batteries do not discharge at 100% efficiency. Energy in excess of the requirement must be held in the battery at the time of discharge. This discharge efficiency is assumed at 95% with current technology. Thus 1967 kW-hr is derived from 1495 kW-hr/0.8/0.95. Improved excess discharge capacity and efficiency are considered in the EEC&S weight analysis.

Error! Reference source not found. shows that batteries and a liquid H_2 feed PEM fuel cell would be about the same weight, while the battery solution is lower weight than that of a compressed H_2 feed PEM fuel cell. Future projections for fuel cells indicated ~ 2x improvements in stack power density and H_2 storage density, while 5 to 10 x improvements are projected for battery technology. Thus the trade will be even more favorable for batteries with future technology and battery energy storage is selected over H_2 feed PEM fuel cell energy storage.

Table 4 provides the weight analysis for the balance of the electric drive system. Estimates have been made for current component performance, mid-term (10 year horizon) and long-term (20 year horizon) project component performance, where the mid-term performance is just the average of the current performance and long-term projected performance (for the motor and motor drive). The 20 year horizon for the motor and motor drive are based on the goals for an ongoing NASA high density 1 MW motor program (8 hp/lbm). Thus, there is no separate motor drive for the 20 year horizon system.

Table 4: Electric Energy Storage and Conversion System Weight

Time Horizon	20	10	current
Component Performance			
Motor			
Power Density (kW/lbm)	5.96	3.98	2.00
Efficiency	0.96	0.94	0.92
Bi-Directional Converter			
Power Density (lbm/kW)	0	0.33	1
Efficiency	1	0.98	0.96
Feeders			
Voltage	1080		
Length (ft)	50		
Efficiency	0.99	0.99	0.99
Energy Storage			
Energy Density (W-hr/kg)	1000	600	200
Efficiency	0.97	0.96	0.95
Max Discharge	90%	85%	80%

Time Horizon	20	10	current
Component Weight			
Motor			
Power (kW)	2102	2102	2102
Weight (lbm)	353	528	1051
Bi-Directional Converter			
Power (kW)	2102	2145	2189
Weight (lbm)	0	715	2189
Feeders			
Current (amps)			
Weight (lbm)	353	530	706
Energy Storage			
Energy (kW-hr)	1713	1832	1967
Weight (lbm)	3768	6719	21641
Total Per Engine (lbm)	**5179**	**10263**	**29533**

B. Thermal Management System

The conceptual design and weight analysis for TMS that services the EES&C system and propulsion system has been completed. As for the EES&C system itself, various technologies have been considered for the TMS. **Error! Reference source not found.** provides the basic TMS architecture along with the system flow rates and temperatures for the hot day takeoff design point. Hot day takeoff has the highest ambient conditions coupled with the highest system heat loads. The coolant loop (bottom left) provides cooling flow to the battery (Bat) and motor drive (MD). The primary architecture driver is the battery coolant maximum temperature limit, set at 140 ºF. Hot day fuel temperature is 120 ºF, and with the limited flow rate of 1.1 lbm/s, even the small load imposed by the mechanically driven fuel pump (21 kW) heats the fuel to 153 ºF, making it unsuitable as a heat sink for the battery coolant. The coolant loop is cooled with Ram Air (the only suitable heat sink as the engine fan air is 178 ºF) at the Ram Coolant Cooler (RCC). The propulsion system heat loads are cooled by the oil loop (center right), which include the accessory gearbox, GTF fan drive, GTF bearings, high spool starter generator, and the low spool motor/generator. All loads are serviced in parallel. The oil is cooled first at the fuel oil cooler (FOC), rejecting as much heat as possible to fuel and the remaining heat is rejected at the air oil cooler (AOC) to fan air. This is desirable as hot fuel has a thermodynamic benefit to the engine cycle and the more heat rejected to fuel, the less heat that is rejected to the AOC, resulting in lower overall heat exchanger weight and lower required fan air for lower fan stream losses (which have to be overcome with more propulsor fan power).

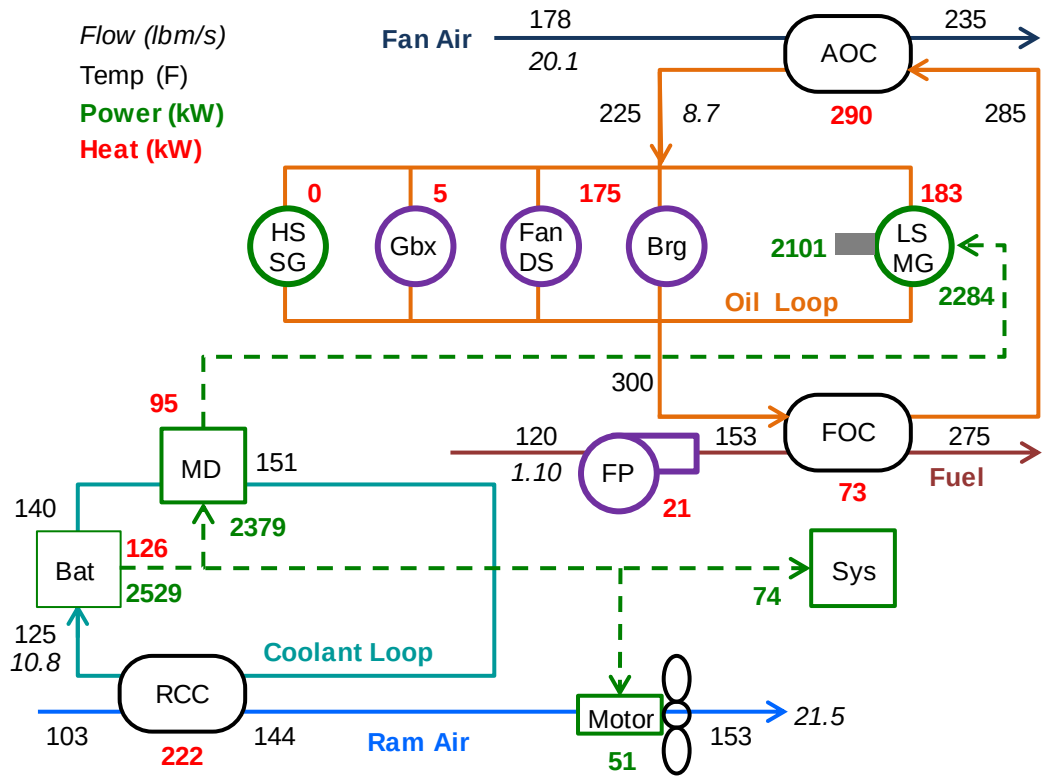

Figure 6: TMS Architecture and Design Condition State Points for Current Horizon Component Efficiencies and Temperature Capability

The heat loads, flow rates, and temperatures shown in **Error! Reference source not found.** are for the current component efficiencies from Table 4. With the battery maximum coolant temperature set at 140 ºF, 21.5 lbm/s of ram air is required to cool the coolant loop. With little ram recovery pressure during takeoff, a 51 kW fan is required to pull the air through the AOC, which adds a load to the battery. Considering the 2379 kW propulsor motor drive load, the 74 kW systems load, the 51 kW ram fan load, and a feeder efficiency of 0.99, 2529 kW is required at the battery output. At 95% efficiency, 126 kW of heat is rejected to coolant by the battery. At 96% efficiency, the motor drive rejects 95 kW of heat to coolant. This heat load drives the need for 21.5 lbm/s of ram air.

At 1.1 lbm/s and a maximum temperature of 275 ºF, there is 94 kW of heat rejection capacity in the fuel. 21 kW of this capacity is consumed by the mechanically driven fuel pump, leaving 73 kW of heat rejection from the

propulsion system oil loop to fuel at the FOC. At 92% efficiency, the LS motor/generator rejects 183 kW to oil. This load, along with the other engine loads sums to 363 kW. With 73 kW rejected at the FOC, the remaining 290 kW is rejected at the AOC, driving the need for 20.1 lbm/s of fan air.

The heat exchangers and motor driven fan have been sized for the current component horizon. **Error! Reference source not found.** (first data column) provides the weight and required heat sink flow results. The RCC at 309 lbm, represents over 80% of the total TMS weight. This is due to the relatively low maximum battery coolant temperature of 140 ºF, which is relatively close to the available ram heat sink temperature of 103 ºF. **Error! Reference source not found.** provides the impact on AOC weight (and fan power) as the battery maximum coolant temperature is increased to 180 ºF, which represents an increase in battery performance. Increasing this temperature by 20 ºF drops the RCC weight by 50%.

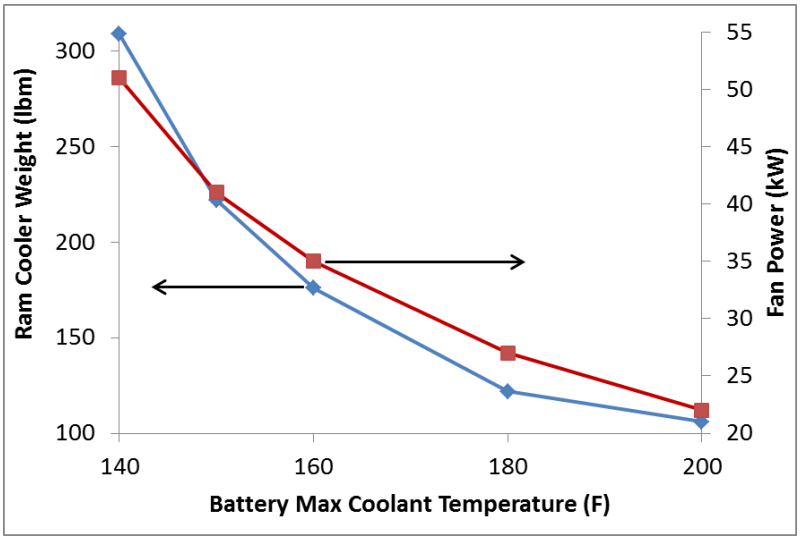

Figure 7: RCC Weight and Ram Fan Power Draw versus Battery Temperature Capability

Other technologies that could decrease the TMS weight include electric engine accessories and high temperature fuel. Mechanically driven fuel pumps operate at a fixed gear ratio to the engine high spool, producing flow far in excess of the demand for most operating conditions. Fuel flow in excess of demand is circulated around the pump and back into the inlet, resulting in a very low pump efficiency and high heat rejection to fuel. A variable speed electrically driven pump would be controlled to deliver only demand flow, and thus have a high efficiency and low heat rejection to fuel. High temperature capable fuel (345 ºF) and oil (350 ºF) enable higher heat rejection to the relatively light FOC, reducing the size and fan air flow required at the AOC. **Error! Reference source not found.** shows the heat loads, ram flow rate and fan air flow rates, for a TMS incorporating high temperature fuel, an electrically driven demand fuel pump and 160 ºF maximum battery maximum coolant temperature, with 10 hear horizion component efficiencies. The fourth data colum of Table 5 provides the corresponding component weights and ram and fan air flow rates. Compared to the current horizion (data colum 1), the combined FOC & AOC weight is decreased by 55% and ram flow and fan flow are decreased by 53% and 69% respectively. **Error! Reference source not found.** also provides the TMS weights, ram air flow rates and fan air flow rates for the current, mid-term 10 year horizon and long-term 20 year horizon component efficiencies with various combinations of electric demand fuel pump, high temperature fuel and high temperature battery technologies.

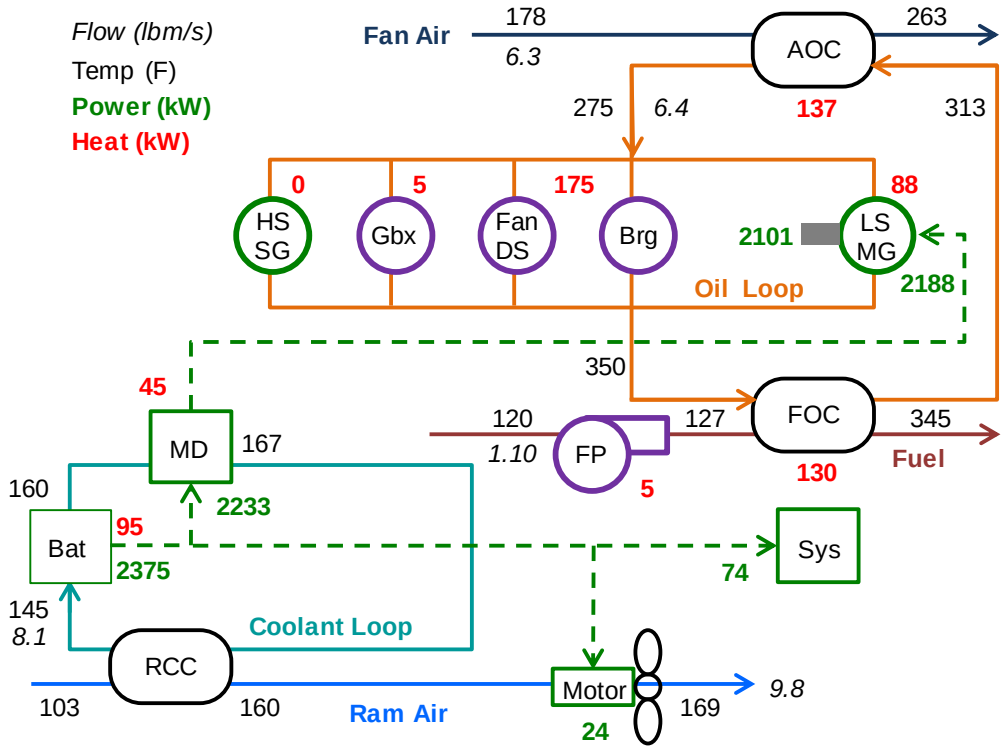

Figure 8: Design Condition State Points for 10 year Horizon Component Efficiencies with High Temperature Fuel Capability and Electric Fuel Pump Technology and High 160 ºF Battery Coolant Capability

Table 5: TMS Air Flow & Weights

	Current	Current*	10 Year*	10 Year*,#	20 Year*	20 Year*,#
Battery Heat (kW)	126	126	95	95	68	68
Motor Drive Heat (kW)	95	95	45	45	0	0
LS Motor/Gen Heat (kW)	183	183	88	88	43	43
Max Coolant Temp (F)	140	140	140	160	140	160
Max Fuel Temp (F)	275	345	345	345	345	345
Ram Air Flow (lbm/s)	21	21	15	9.8	9.1	5.4
Fan Air Flow (lbm/s)	20	10	6.3	6.3	4.7	4.7
RCC Weight (lbm)	309	309	181	105	78.6	50
FOC Weight (lbm)	5	8	9	9	10	10
AOC Weight (lbm)	51	27	16	16	11	11
Ram Fan Weight (lbm)	26	26	18	12	11	7
Total (lbm)	**391**	**369**	**224**	**143**	**111**	**78**

* includes high temp fuel and electric fuel pump
\# includes 160 ºF maximum battery coolant temperature (as opposed to 140 ºF maximum battery coolant temperature)

V. Benefits

As discussed in the "Study Baseline Vehicle and Engine" Section 2.0, the baseline vehicle is the N+4 2035 "Refined SUGAR" airframe powered by a second generation conventional GTF engine. The hybrid electric vehicle alternative replaces the cGTF with and hGTF, and adds the weight difference of the hGTF propulsion system (compared to the cGTF), and the EES&C system and TMS weight. The analysis is executed for a fixed vehicle (both vehicles are held at the same TOGW), so as weight is added, fuel carrying capacity is reduced. Thus, the thrust requirements are the same for both the cGTF and hGTF engines.

Alternatively, a rubber vehicle model could be used (TOGW allowed to grow) such that each vehicle is sized to provide the same maximum range for the capability mission. The process for determining the overall fuel burn and energy consumption benefit requires an iterative analysis. First, thrust requirements are selected for the hGTF engine. The engine is sized for cruise, the LS motor/generator, EES&C system power and energy requirements are determined, and the systems are sized. The hGTF aircraft is then flown through the capability mission to determine the total mission. If the range requirement is not met, the vehicle is upsized and new thrust requirements are selected. The above process is iterated until convergence is achieved. As implied in the EES&C system and TMS weight analysis above, the weight of these systems is very uncertain and will be decreasing as new technology matures. Thus, the fixed vehicle model has been run parametrically, with added weight as an independent variable.

Figure 9 provides the results of the mission vehicle analysis. The hGTF reduces Jet-A fuel burn both during cruise due to the improved engine TSFC, and during takeoff and climb as stored electric energy is providing some of the shaft power to drive the fan. Consider first Figure 9a, which provides the capability mission range of the hGTF vehicle compared to the cGTF vehicle (3300 nm). If the hGTF implementation comes with no weight increase (no added weight for the electric energy storage and conversion (EES&C) system, thermal management system (TMS) or the LS motor), a 200 nm range benefit is realized. As weight is added, fuel is displaced on the fixed vehicle and range is decreased. The figure shows that the hGTF vehicle provides a capability range benefit only if the added weight is less than 1200 lbm. Some compromise on capability mission range may be acceptable if the DOC mission fuel burn reduction is judged significant.

Consider now Figure 9b, which provides the 900 nm DOC mission fuel burn of the hGTF vehicle compared to the cGTF vehicle (6630 lbm). Again, if the hGTF implementation comes with no weight increase, a 580 lbm fuel burn benefit is realized. As weight is added, fuel must be added to carry the weight. The figure shows that the hGTF vehicle provides a DOC mission fuel burn benefit all the way up to an added weight of ~ 16000 lbm.

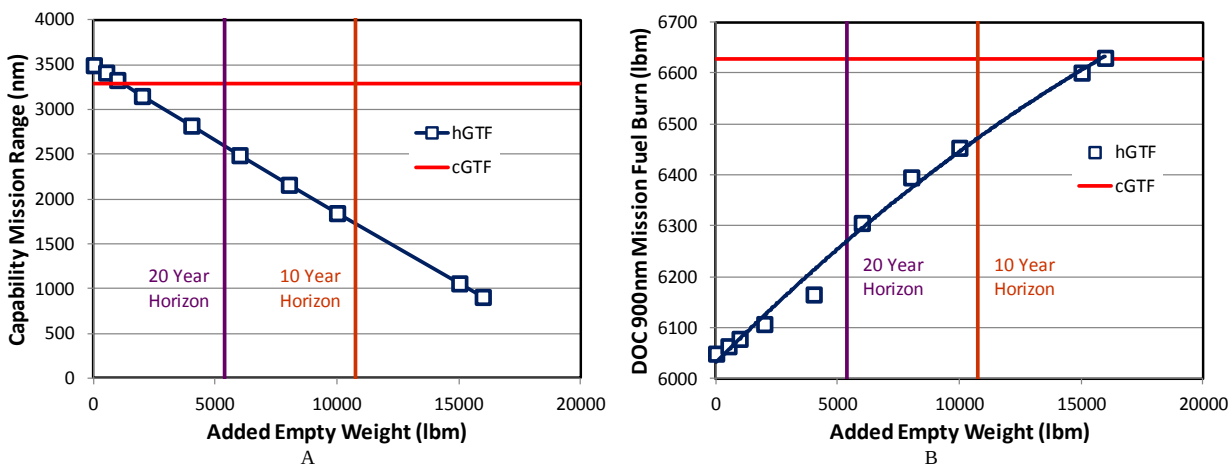

Figure 9: Range and Fuel Burn Benefits for the hGTF Based Aircraft at 10 and 20 Year Technology Horizons

Also shown on Figure 9 are estimates of the EES&C system, TMS and LS motor at various technology levels. At the most aggressive technology horizon, the total weight increase of the hGTF system is estimated at ~ 5400 lbm. The hGTF vehicle suffers from a 690 nm_(21%) range decrease for the capability mission at this weight, but can provide a 360 lbm (5%) Jet-A fuel burn decrease for the DOC mission.

This Jet-A fuel burn decrease includes "free" energy in the batteries charged on the ground. The equivalent Jet-A fuel burn to provide 1495 kW-hr, at the typical electric power specific fuel consumption of a large gas turbine engine operating at a peak thermal efficiency (~ 0.27lbm/hr/kW) is ~ 400 lbm, approximately the same as the in air Jet-A fuel burn reduction. Figure 10 shows the fuel burn with the fuel consumption for ground charging included (green line). Thus accounting for the ground energy consumption/CO_2 emissions, the hGTF aircraft at the 20 year technology horizon is approximately energy consumption/CO_2 emissions neutral compared to cGTF aircraft.

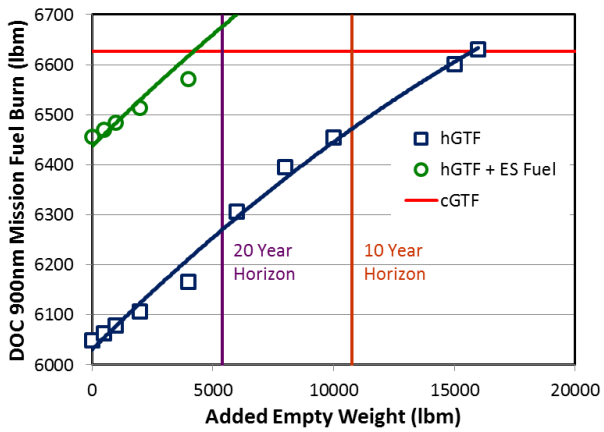

Figure 10: Fuel Burn (Including both Airborne and Ground) Benefits Analysis for the hGTF Based Aircraft at 10 and 20 Year Technology Horizons

VI. Conclusion

This study has investigated the potential benefits of using stored electric power to provide boost power, through a low spool mounted motor, for an engine core sized and optimized to provide maximum cruise thrust. Such an hGTF propulsion system provides a modest improvement in cruise TSFC, 2.3 %, but has an aircraft level power deficit of 4.2 MW at take-off. With aggressive assumptions for future battery, electric system and thermal management system weight and performance, it has been shown that a 5% reduction in aircraft 900 nm DOC mission fuel burn is possible. However, with the fuel burn required to charge batteries is included, there is no fuel burn reduction.

This improvement alone is not enough to motivate a radical change in propulsion system technology. If community noise becomes a major issue, this approach can substantially reduce taxi-way noise through the electric taxi operating mode. In addition, the study does highlight that there is a hybrid gas-electric system architecture that can provide both an aircraft and overall (including fuel for battery charging) fuel burn benefit. Thus, future study in other alternative architectures [4,5] is recommended.

Acknowledgments

The material provided in this document is based upon work supported by the National Aeronautics and Space Administration under Contract Number NNC14CA32C.

Any opinions, findings and conclusions or recommendations expressed in this material are those of the author(s) and do not necessarily reflect the views of the National Aeronautics and Space Administration.

The authors wish to acknowledge Dan Kupratis and Bob Bengtson from Pratt & Whitney and Pedro Canache and Bill Wicklund from United Technologies Aerospace Systems for the technical support in this research.

References

[1]Bradley, M. K., and Droney, C. K., "Subsonic Ultra Green Aircraft Research Phase I Final Report," National Aeronautics and Space Administration Contractor Report NASA/CR–2011-216847, 2011.

[2]Bradley, M. K., and Droney, C. K., "Subsonic Ultra Green Aircraft Research Phase II: N+4 Advanced Concept Development," National Aeronautics and Space Administration Contractor Report NASA/CR-2012-217556, 2012.

[3]Rheaume, J. M., "Energy Storage for Commercial Hybrid Electric Aircraft," *SAE 2016 Aerospace Systems and Technology Conference*, SAE Hartford CT (submitted for publication)

[4]Welstead, J.R. and Felder, J.L., "Conceptual Design of a Single-Aisle Turboelectric Commercial Transport with Fuselage Boundary Layer Ingestion," *AIAA SciTech Conference*, American Institute of Aeronautics and Astronautics, San Diego, CA, 2016, AIAA-2016-1027

[5] Jenson, R.H., Brown, G.V., Felder, J.L. and Duffy, K. P. "Turboelectric Aircraft Drive Key Performance Parameters and Functional Requirements," *AIAA Propulsion and Energy Conference*, American Institute of Aeronautics and Astronautics, Orlando, FL, 2015, AIAA-2015-3890